IEEE Access
Multidisciplinary ⋮ Rapid Review ⋮ Open Access Journal

Received 2 July 2024, accepted 31 July 2024, date of publication 5 August 2024, date of current version 15 August 2024.

Digital Object Identifier 10.1109/ACCESS.2024.3438242

RESEARCH ARTICLE

EVs in Distribution Networks–Optimal Scheduling and Real-Time Management

DESPOINA KOTHONA[1], (Student Member, IEEE), ANESTIS G. ANASTASIADIS[2], KOSTAS CHRYSAGIS[2], GEORGIOS C. CHRISTOFORIDIS[1], (Senior Member, IEEE), AND AGGELOS S. BOUHOURAS[1], (Member, IEEE)

[1]Department of Electrical and Computer Engineering, University of Western Macedonia, ZEP Campus, 501 00 Kozani, Greece
[2]Public Power Corporation S.A., 104 32 Athens, Greece

Corresponding author: Despoina Kothona (d.kothona@uowm.gr)

ABSTRACT The high penetration of Renewable Energy Sources (RES) and Electric Vehicles (EVs) into the grid introduces new challenges for Distribution Systems (DSs). The uncertainties related to these assets necessitate the development of real-time methodologies to optimize the operation of Low Voltage (LV) and Medium Voltage (MV) DSs. This paper aims to fill the gap in the literature by proposing a holistic real-time DS optimization model that considers the coupling of MV and LV DSs. Specifically, the methodology adopts a bottom-up three-layer approach. At the first layer an optimal EV Smart Charging Scheduling (SCS) methodology is applied for power losses minimization at the LV DSs, considering the characteristics of individual households (maximum rated power of the electrical installation, Photovoltaic generation, and load and EV charging demand). The second layer introduces a residential controller that fully exploits the flexibility of EVs, minimizing the impact of forecasting errors while satisfying limitations regarding households' overloading protection. The third layer involves a real-time Network Reconfiguration (NR) methodology, considering real-time power transactions between MV and LV DSs, and determining the optimal topology through a cost-worth analysis of power loss reduction and switch operation costs. The overall design of the proposed methodology ensures broader adoption, repeatability, adaptability, and scalability across diverse DSs, including various types of LV DSs (residential, commercial, etc.) and different MV DS configurations. The proposed methodology can reduce DS power losses by up to 34.41% compared to the base scenario, which involves the operation of the DS without employing either EV SCS or NR.

INDEX TERMS Distribution system, electric vehicle charging, vehicle-to-grid, forecast uncertainty, real-time energy management.

NOMENCLATURE

Abbreviations

EU	European Union.
MV	Medium Voltage.
LV	Low Voltage.
DS	Distribution System.
DR	Demand Response.
DSO	Distribution System Operator.
EV	Electric Vehicle.
LSTM	Long Short-Term Memory.
MAE	Mean Absolute Error.
MARNE	Mean Absolute Ranged Normalized Error.
NLP	Non-Linear Problem.
NRMSE	Normalized Root Mean Square Error.
NA	Not Applicable.
MPC	Model Predictive Control.
NR	Network Reconfiguration.
PF	Power Flow.
PV	Photovoltaic.

The associate editor coordinating the review of this manuscript and approving it for publication was Behnam Mohammadi-Ivatloo.

SoC	State of Charge.
SCS	Smart Charging Scheduling.
RES	Renewable Energy Sources.

Sets

i, j / m, n	Sets of buses for LV / MV network.
l	Set of the system's lines.
k	Set of EVs/households connected at each bus.

Parameters

$g_{m,n}$, $r_{i,j}$, $x_{m,n}$	Conductance, resistance and reactance of line connected from bus i/m to bus j/n.
N	Number of buses at MV DS.
$P^{PV,pred}_{t,i,k}$, $P^{load,pred}_{t,i,k}$	Predicted PV power and load demand of k^{th} household connected to bus i at time t.
$P^{PV,real}_{t,i,k}$, $P^{load,real}_{t,i,k}$	Real PV power and active power demand of k^{th} household connected to bus i at time t.
$Q^{load,real}_{t,i,k}$	Real reactive power demand of k^{th} household connected to bus i at time t.
$\text{pf}_{i,k}$	Power factor of k^{th} household connected to bus i.
$P^{nom}_{i,k}$	Nominal power of k^{th} house connected to bus i.
$P^{ev,adj}_{t,i,k}$	Adjusted power of k^{th} EV connected to bus i at time t.
η_{ch}, η_{dis}	Charging and discharging efficiency of EVs.
$\text{Cap}_{i,k}$, $\text{SoC}^{\max}_{i,k}$	Battery capacity and maximum SoC of k^{th} EV connected to bus i at time t.
$T^{dep}_{i,k}$	Departure time of k^{th} EV connected to bus i.
C^{en}, C^{s}	Energy and switching action cost.
s^{init}_{l}	Binary parameter to define the initial state of the MV DS, i.e., is equal to 1 if the line is in service.

Real Variables

$P_{t,i,j}$, $Q_{t,i,j}$	Real and reactive power flow at LV DS from bus i to bus j at time t.
$V_{t,i}$	Voltage magnitude at time t at bus i.
d_m	Argument of voltage at bus m.
$P^{MV}_{m,n}$	Power flow at MV DS from bus m to bus n.
$P^{ev}_{t,i,k}$, $E^{ev}_{t,i,k}$	Charging/Discharging power and energy of k^{th} EV connected to bus i at time t.
P^{LV}_{m}	Total power generation/demand of LV DS connected to bus m of the MV DS.
$P^{gen,MV}_{m}$	Power generated at bus m of MV DS.

Non-Negative Variables

$P^{ev,ch}_{t,i,k}$, $P^{ev,dis}_{t,i,k}$, $\text{SoC}_{t,i,k}$	Charging power, discharging power and SoC of k^{th} EV connected to bus i at time t.
P^{loss}	Power losses at MV DS.

Binary Variables

a_l	Binary variable that is equal to 1 if the state of the line changes between two iterations.
s^{bin}_{l}	Binary variable that is equal to 1 if the line is on service after the reconfiguration.
$s_{m,n}$	Binary variable that is equal to 1 if buses m and n are connected.

I. INTRODUCTION

In response to the instability observed in energy prices, the European Commission announced Regulation 2022/1854 [1], which requires the Member States to take actions to reduce power consumption during peak hours by at least 5%. This mandatory peak reduction aligns with the EU's efforts to enhance the efficient operation of DSs, with a particular focus on reducing power losses [2]. A report published by the Council of European Energy Regulators [3] highlights that power losses represent a substantial portion of the overall energy. According to the 2nd CEER Report on Power Losses, published by the Council of European Union Regulators in 2020, distribution losses in the majority of member state countries constitute more than 2% of the annual injected energy [3]. As highlighted in the report of distribution tariff methodologies in Europe [4], the cost of the energy losses can be directly transferred to the consumers as a distribution tariff, or it can be included in the bidding energy price in the energy markets. Therefore, the reduction of power losses can directly contribute to alleviating energy prices.

Despite the effort of EU to enhance the efficiency of DSs, the insight of EU towards the decarbonization of energy [5] and transport sectors has altered the load profile of DSs. Hence, DSs are currently facing significant challenges. On the one hand, the lack of synchronization between the demand of EVs and the generation of RES affects the power quality of the system. On the other hand, these new assets are characterized by high uncertainty. The dependence of RES on meteorological conditions and the uncertainty associated with EV charging profiles result in high deviations between forecasts and actual generation/demand values, impeding the day-ahead scheduling of DSs' operation.

To address these challenges and achieve the objectives of the EU, there has been significant attention towards the development of EV SCS [6] and the application of NR schemes. Implementing these schemes could lead to deferral investments and enhanced efficiency and reliability for DSs [7]. However, their successful implementation requires consideration of several factors. Firstly, uncertainties related to RES

generation, load demand, and EV charging profiles (time of arrival, SoC, time of departure) should be managed in real or near-real time. This approach enhances the robustness of SCS by mitigating the impact of forecasting errors. Additionally, according to the latest ''Global EV outlook'' published by the International Energy Agency (IEA), most charging demand is currently met by residential chargers. Therefore, the limitations of residential charging infrastructure, such as overload protection and maximum charging power, must be addressed concurrently with operational constraints of DS. Finally, the coupling of MV and LV DSs should be considered to optimize the performance of DS by leveraging both the flexibility provided by the EVs and the benefits of NR.

A. LITERATURE REVIEW

The charging scheduling methodologies proposed in the literature focus on various objective functions. Some studies have proposed multi-objective optimization methods. For instance, the authors in [8] aimed to minimize both electricity consumption cost and battery degradation cost, while the authors in [9] proposed a method to minimize charging cost and cost of power losses. Other studies directly addressed the concerns of DSOs related to the DS operational characteristics. For example, the authors in [10] proposed a voltage control strategy, and [11] focused on transformer loading. Furthermore, [12] addressed the minimization of power losses. However, recent papers have shifted focus towards minimizing charging costs [13], [14]. The authors in [15] and [16] proposed an EV SCS method using TOU scheme, while the authors in [17] and [18] examined the impact of dynamic energy pricing in charging scheduling.

Aside from the objective function, the proposed methodologies differ in terms of the DS voltage level and the charging infrastructure they refer to. Most papers focused on the impact of SCS on MV DS considering the existence of charging stations. The authors in [19] examined the effect of coordinating charging stations in specific buses of the IEEE 33-bus system. The same DS was also examined in papers [20], [21], and [22]. Apart from charging stations connected to MV DS, residential charging infrastructure in LV DS was also considered. For example, the authors in [8] examined peak shaving through charging scheduling in a LV DS in Sydney, while the authors in [23] investigated voltage stability and power losses in a LV DS in Greece. A different approach was presented in [24] where the authors focused on the effect of SCS in a microgrid.

The aforementioned papers primarily focused on day-ahead applications, which require predictions of various factors. For charging cost minimization problems, these predictions typically involve factors such as time-of-arrival, time-of-departure, SoC of EVs, aggregated load forecasts, and predictions of RES power generation, as discussed in [11] and [15]. However, in more complex scenarios where charging scheduling directly addresses DS power quality, such as voltage control and power losses reduction, individual load forecasts for each node of the system should also be considered [12]. In such cases, the uncertainty of load forecasting may increase due to end-user stochasticity, particularly in residential load contexts. For the latter it is crucial to note that forecasting errors may lead to violations of the limitations of residential charging infrastructure, i.e., overloading protection issues.

To address these uncertainties, methodologies for real or near-real time SCS have been proposed in [20], [21], [24], [25], [26], and [27]. In [20], a real-time model was proposed to minimize the carbon emissions, while [25] focused on minimizing customer's cost and maximizing the use of EV battery. Additionally, [26] aimed to minimize the difference between real-time load demand or generation and the commitment value. Moreover, [27] introduced a real-time control charging strategy at a charging hub to minimize the EV charging cost. In [24], the authors focused on developing a demand-response-based energy management method that included EVs in the optimization problem. The model's objective was the minimization of CO_2 emissions, generation cost and battery degradation. A different approach was proposed in [21] combining both day-ahead and real-time SCS using a bi-layer approach. The day-ahead scheduling aimed to maximize the load margin index, while the real-time scheduling aimed to minimize the cost of EV aggregation.

In these papers the authors applied the SCS methodologies either on MV or LV DSs, without considering the benefits of NR. Few methodologies in the literature have combined both NR and EV SCS. However, existing methodologies mainly focus on the day-ahead scheduling [12], [22], [28], [29] and their effectiveness is questioned in real-applications. Therefore, real-time methodologies combining both EV SCS and NR are essential to be developed. This integration is essential because power transactions between coupled LV-MV DSs are required to determine the optimal system topology under NR scheme. Otherwise, any deviation between forecasted and real values could significantly impact the optimal topology of the system.

B. SCOPE OF WORK AND CONTRIBUTIONS

The literature review is summarized in Table 1. Despite the progress made, several gaps can be identified:

- Real-time methodologies considering the coupling between MV and LV DS and integrating both NR and SCS have not been examined yet.
- Previous research primarily focused on charging stations, with limited consideration of technical constraints of residential charging infrastructure, i.e., overloading protection in households [8], [12], [16], [23].
- Uncertainties related to RES power generation and load demand forecasts were often overlooked, resulting in inefficiencies in large-scale systems.
- Power loss minimization in real-time applications has also been neglected, despite its potential to reduce electricity costs and provide valuable insights to DSOs

TABLE 1. Literature review.

Ref.	OF	System level	Coupling of LV and MV DSs	NR	EVs charging/ discharging scheduling	RES	Time of arrival uncertainties	Load demand and/or generation forecast uncertainties	Overloading protection of residential chargers
[8]	Minimizing electricity cost and battery degradation cost	LV	No	NA	Day-ahead	Yes	Yes	Yes	No
[9]	Minimizing charging cost and cost of power losses	MV	No	No	Day-ahead	No	No	No	NA
[10]	Voltage control	MV	No	No	Applicable in near real-time	No	No	No	NA
[11]	Transformer loading	LV	No	No	Day-ahead	No	No	No	No
[12]	Minimizing power losses	MV+LV	Yes	Yes	Day-ahead	No	No	No	No
[13]	Minimizing electricity cost	MV	No	NA	Day-ahead	Yes	Yes	Yes	NA
[14]	Minimizing electricity cost	Charging station	No	NA	Day-ahead	Yes	Yes	Yes	NA
[15]	Minimizing charging cost	LV	No	NA	Day-ahead	No	Yes	Yes	No
[16]	SCS methodology based on EV owner interest and grid impact (voltage drop and transformer loading)	LV	No	NA	Real-time	Yes	Yes	Yes	No
[17]	Minimizing charging cost	Charging station	No	NA	Day-ahead	No	No	No	NA
[18]	Minimizing charging cost and phase unbalance	LV	No	NA	Day-ahead	No	No	Yes	No
[19]	Minimizing generation, dispatching and wholesale marker cost	MV	No	No	Day-ahead	Yes	Yes	Yes	NA
[20]	Minimizing carbon emissions	MV	No	No	Real time	Yes	Yes	Yes	NA
[21]	Minimizing operation cost of EV aggregators	MV	No	No	Bi-layer	No	Yes	No	NA
[22]	Maximizing profit and buyers' satisfaction, minimizing power losses and purchase cost	MV	No	Yes	Day-ahead	No	No	No	NA
[23]	Minimizing power losses	LV	No	No	MPC	No	No	No	No
[24]	Minimizing CO_2 generation cost and battery degradation	Microgrid	No	NA	Real-time	Yes	Yes	Yes	No
[25]	Minimizing consumer's cost and maximizing EV battery utilization	Individual EV	No	NA	Real-time	No	Yes	No	No
[26]	Minimizing the difference between real-time consumption/production and the commitment value	MV+LV	Yes	No	Applicable in near real-time	Yes	Yes	Yes	No
[27]	Minimizing charging cost	Charging hub	No	NA	Real-time	No	Yes	Yes	NA
[28]	Minimizing fuel and energy cost and cost of incentive paid to customers for participating in the DR	MV	No	Yes	Day-ahead	Yes	No	No	NA
[29]	Maximizing daily profit	MV	No	Yes	Day-ahead	Yes	Yes	Yes	NA
This paper	Minimizing power losses at LV DS; Minimizing power losses and switching cost at MV DS	MV+LV	Yes	Yes	Real-time	Yes	Yes	Yes	Yes

for incentivizing EV participation in charging control schemes.

This paper addresses these gaps and proposes a coupled MV-LV optimization model for real-time power loss minimization. The proposed model comprises three layers. The first layer focuses on EV SCS at residential charging infrastructure, aiming to minimize power losses in LV DS. The SCS methodology employs model predictive control considering not only uncertainties of EVs, i.e., time-of-arrival and SoC but also forecasting errors of RES generation and load demand. Forecasts of RES generation and household demand are updated every 15 minutes using a LSTM model. Also, the EV SCS considers the limitations of household overloading protection. At the second layer,

a residential controller adjusts the charging power of each EV in real-time. This adjustment considers deviations between real measurements and predicted values of load demand and RES generation, as well as the constraints posed by household overloading protection. Finally, the third layer involves a real-time NR reconfiguration at MV DS, considering real-time power transactions between MV and LV DSs. The main objective is to define the optimal topology of the MV DS through a cost-benefit assessment that weighs the profit of reducing power losses against the switching costs associated with NR.

In this context the contributions of this work aim to:

- Fill the gap in the literature regarding a holistic real-time DS optimization model that considers the coupling of MV and LV DSs. The proposed methodology employs a bottom-up approach that optimizes the DS considering: a) the needs of individual residences (load demand, PV generation and EV charging demand), b) the technical characteristics of LV and c) the technical characteristics of MV DS.
- Propose a residential controller that fully-exploits the flexibility of EVs. The controller deals with forecasting errors related to RES generation, while ensuring compliance with household overloading protection limits.
- To serve as a basis for future research into designing price incentives to encourage EV owners to participate in Smart Charging System (SCS) schemes.
- Ensure the methodology's broader adoption, repeatability, adaptability, and scalability across diverse DSs. This includes various types of LV DSs (residential, commercial, etc.) and different configurations of MV DSs.

II. METHODOLOGY

A. FORECASTING MODEL

Several PV and load demand forecasting models have been proposed in the literature, dealing with different forecasting horizons, i.e., very short-term, short-term and long term. However, as the forecasting horizon increases, deep learning methods outperforms many well-known machine learning and statistical methods [30]. Therefore, in this paper, the LSTM model is selected to generate forecasts for both RES generation and load demand of each household for the next day, with a 15-min resolution. The selection of the LSTM model is based on its ability to capture dependencies among the input variables and retain crucial information from previous time-steps to predict the next ones. For the development of the LSTM the sliding window method is utilized, which is crucial in energy management applications that involve load and RES generation predictions, as it updates the predictions and alleviates the forecasting error by capturing load demand and generation patterns [31].

B. 1ST LAYER: EV SMART CHARGING SCEDULING AT LV DS

The EV SCS model is formulated as an NLP problem and is applied to LV DS aiming to minimize power losses, as presented in (1). For the PF analysis, the linear DistFlow is employed, as expressed in (2) – (4). The linear DistFlow is the most appropriate choice for real time applications in LV DSs due to its computational efficiency and the relatively low deviation compared to generic NLP AC PF [32]. Additionally, the voltage thresholds of each bus at time t should be within the acceptable limits, as defined in (5).

$$\min OF_{LV} = \sum_{t=0}^{T} \sum_{i=0}^{B} \sum_{i=0}^{B} \left(r_{i,j} \cdot \left(P_{t,i,j}^{2} + Q_{t,i,j}^{2} \right) \right) \tag{1}$$

$$P_{t,i,j} = \sum_{b=0}^{B} P_{t,j,b} + \sum_{k=0}^{K} \left(P_{t,j,k}^{load,pred} - P_{t,j,k}^{PV,pred} + P_{t,j,k}^{ev} \right) \tag{2}$$

$$Q_{t,i,j} = \sum_{p=0}^{B} Q_{t,j,p} + Q_{t,i,k}^{load,real} \tag{3}$$

$$V_{t,i} = V_{t,j} - 2 \cdot \left(r_{i,j} \cdot P_{t,i,j} - x_{i,j} \cdot Q_{t,i,j} \right) \tag{4}$$

$$V^{min} \leq V_{t,i} \leq V^{max} \tag{5}$$

The constraints of the EVs are presented in (6) – (14). Specifically, (6) models the overloading protection of the household. According to this, the total household load demand and charging power of the EVs cannot exceed the rated capacity of the installation. Therefore, the charging/discharging power of the EV is defined considering the PV power generation and the load demand. In (7) the energy capacity of the k^{th} EV connected at bus i at time t ($E_{t,i,k}^{ev}$) is estimated regarding the variables $P_{t,i,k}^{ev,ch}$ and $P_{t,i,k}^{ev,dis}$ defined in (8). These variables are both positive and are used to define the charging and discharging power, respectively. Additionally, (9) is used to ensure that $P_{t,i,k}^{ev,ch}$ and $P_{t,i,k}^{ev,dis}$ do not take positive values concurrently. Moreover, constraints (10) and (11) define the estimation of the SoC and the constraints regarding its limits. The proposed SCS methodology has been developed considering the preferences of EV owners regarding the time-of-departure and the SoC at the time of their departure. Yet the latter depends on the limitations of the electrical installation. These are expressed in (12) which ensures that the EV battery will reach the maximum SoC by the time of departure ($t = T_{i,k}^{dep}$).

$$P_{t,i,k}^{load,pred} - P_{t,i,k}^{PV,pred} + P_{t,i,k}^{ev} \leq P_{i,k}^{nom} \tag{6}$$

$$E_{t,i,k}^{ev} = \eta_{ch} \cdot P_{t,i,k}^{ev,ch} - \frac{1}{\eta_{dis}} P_{t,i,k}^{ev,dis} \tag{7}$$

$$P_{t,i,k}^{ev} = P_{t,i,k}^{ev,ch} - P_{t,i,k}^{ev,dis} \tag{8}$$

$$P_{t,i,k}^{ev,ch} \cdot P_{t,i,k}^{ev,dis} = 0 \tag{9}$$

$$\mathrm{SoC}_{t,i.k} = \mathrm{SoC}_{t-1,i.k} + \frac{E_{t,i.k}^{ev}}{\mathrm{Cap}_{i.k}} \tag{10}$$

$$0.2 \leq \mathrm{SoC}_{t,i.k} \leq 1 \tag{11}$$

$$\mathrm{SoC}_{t=T_{i,k}^{dep},i,k} = \mathrm{SoC}_{i,k}^{\max} \tag{12}$$

C. 2ND LAYER: RESIDENTIAL CONTROLLER

The residential controller operates in real-time, and it is triggered by new measurements of PV generation and load demand. Its primary function is to alleviate the impact of

forecasting errors in LV DSs while concurrently preventing power outages caused by overloading of the electrical installation. This is implemented by dynamically adjusting the charging/discharging power of the EV, considering two distinct conditions which should be satisfied concurrently (Figure 1).

The first condition is used to deal with the PV and/or load forecasting errors in real-time. This is extremely important since the uncertainties related to forecasts in households can cause actual EV power to deviate from the scheduled one, leading to inefficiencies in large-scale systems. Specifically, without addressing these forecasting errors, the real-time operation of the system would significantly deviate from the scheduled plan. Therefore, by adjusting the charging/discharging power of the EVs in real time, the total demand of the household can be equal or close to the scheduled one. This also ensures that the adjustment does not violate the constraint set at the first layer, since the scheduled demand should be less than or equal to the nominal rated power of the electrical installation (6). Considering these, in the second condition if the absolute value of a forecasting error exceeds a predefined threshold, then the power of the EV is adjusted to mitigate the mismatch between the real and predicted generation and/or demand, as expressed in (13). This threshold is a user-defined parameter. The higher the threshold, the more tolerant the controller is to forecasting errors.

The second condition pertains to the maximum rated power of the electrical installation of the household, preventing power outages. Specifically, there might be cases where the forecasting error does not exceed the predefined threshold. In such cases the first condition is not checked. Therefore, we should make sure that the EV charging power will be reduced, if the total demand at time t exceeds the maximum power ($P^{nom}_{i.k}$), as defined in (14).

$$P^{ev,adj}_{t,i,k} = P^{ev}_{t,i.k} + P^{load,pred}_{t,i.k} - P^{PV,pred}_{t,i.k} - \left(P^{load,real}_{t,i.k} - P^{PV,real}_{t,i.k}\right) \quad (13)$$

$$P^{ev,adj}_{t,i,k} = P^{nom}_{i,k} - P^{ev}_{t,i,k} \quad (14)$$

D. 3RD LAYER: NR AT LV DS

At the third layer, real-time NR is employed and formulated as a MINLP problem. The MV DS optimization process aims to minimize not only the cost of the power losses but also the cost related to the switching actions through a cost-worth assessment, as indicated in (15).

$$\min\left(OF_{MV}\right) = C^{en} \cdot P^{loss} + C^{s} \cdot \sum\nolimits_{l=1}^{L} a_l \quad (15)$$

To estimate the power losses at the MV DS, DC power flow is utilized, as presented in (16), (17) and (18). The DC PF has been extensively used in unit commitment problems at the transmission systems, due to its computational efficiency and the low deviation compared to AC power flow. Specifically, the results presented in [33] highlighted that the DC PF is

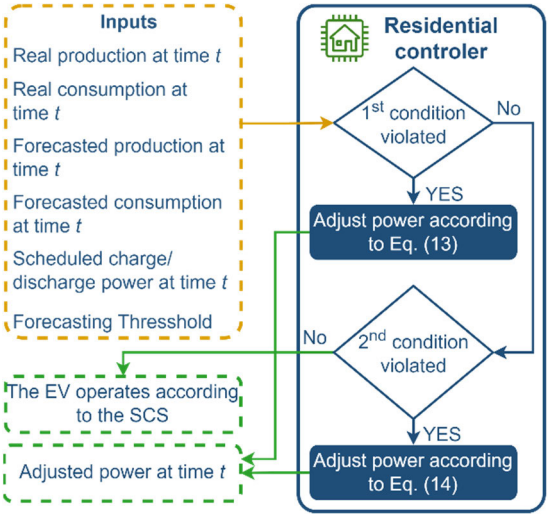

FIGURE 1. Residential controller.

60 times faster than AC. Additionally, the accuracy of DC PF depends on the ratio x/r and increases when r≪x [34]. This limitation makes the DC PF unsuitable for LV DS application. However, in MV DS the ratio x/r is greater than 1 which means that the PF error could be acceptable.

$$P^{loss} = 0.5 \cdot \sum\nolimits_{m=0}^{N} \sum\nolimits_{n=0}^{N} \left(g_{m,n} \cdot (d_m - d_n)^2\right) \quad (16)$$

$$P^{gen,MV}_{m} = \sum\nolimits_{n=0}^{N} P^{MV}_{m,n} + P^{LV}_{m} \quad (17)$$

$$P^{MV}_{m,n} = \frac{1}{x_{m,n}} \cdot s_{m,n} \cdot (d_m - d_n) \quad (18)$$

In (18) the PF of the lines is estimated by considering the binary variable $s_{m,n}$, which defines the topology of the system. To ensure that the topology of the system is valid, two conditions must be ensured: a) the radiality of the MV DS is maintained, and b) all buses are connected to the system. These conditions are formulated in (19), (20) and (21).

$$s_{n,m} = s_{m,n} \quad (19)$$

$$s_{m,n} = s^{bin}_{l}, \quad \forall (m,n) \in l \quad (20)$$

$$\sum\nolimits_{l=1}^{L} s^{bin}_{l} = N - 1 \quad (21)$$

Finally, (22) and (23) are used to define a_l variable. This is a binary variable responsible for tracking the switching actions and is used to estimate the switching cost in (15).

$$a_l \geq s^{bin}_{l} - s^{init}_{l} \quad (22)$$

$$a_l \geq s^{init}_{l} - s^{bin}_{l} \quad (23)$$

E. OVERALL PROPOSED METHODOLOGY

The flowchart presented in Figure 2 outlines the proposed methodology. At each time step t, the LSTM provides the 24-hour predictions for PV power generation and load demand, with a time resolution of 15-min. Based on this temporal granularity, the LSTM provides 96 predicted values, i.e., 96 quarters within the day. It should be noted that the

LSTM is applied to each individual household and is executed each time new measurements are available, based on the sliding window method. The EV SCS employes model predictive control approach [35] and utilizes predictions to define the SCS of EVs. Therefore, the continues update of these predictions through the sliding window method is essential to alleviate the forecasting error and increase the robustness of the SCS.

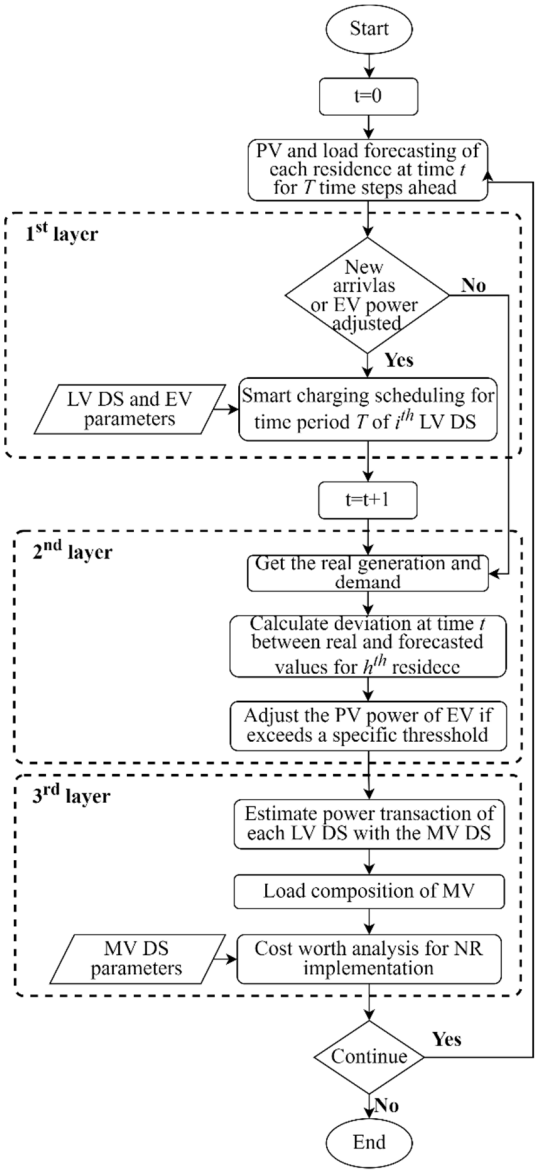

FIGURE 2. Flowchart of the proposed methodology.

Afterwards, the EV SCS is applied at each LV DS, considering the forecasted values of load demand and PV generation of each household. The SCS methodology is triggered at time t so to be updated by two conditions: a) the charging/discharging power of the EV(s) has been adjusted at time t-1 by the residential controller, and/or b) new EVs are plugged-in at time t. The concept here is that every deviation from the initial scheduling caused either by the residential controller or by a new EVs' arrival, affects the optimality of the SCS and therefore an updated optimal schedule should be generated. In this way, the proposed SCS methodology can efficiently deal with the forecasting errors and the uncertainties of EVs, i.e., time-of-arrival and SoC. The EV SCS methodology provides an optimal EV charging plan for the time span $[t + 1, t + 97]$. At the next timestep $(t + 1)$ the residential controller adapts, if it is required, the charging/discharging power of the EVs. In case the latter happens, the EV charging plan is updated, as presented in Case A within Figure 3. If no adjustments are made, the charging plan established at time $t + 1$ is applied, as presented in Case B and Case C within Figure 3. Now, in case new EVs arrive at $t+1$ the SCS is updated (Case B within Figure 3). Otherwise, at $t + 1$ the EV SCS is not updated (Case C within Figure 3).

It should be noted that in all cases presented in Figure 3 the NR is applied in real-time. In many papers NR methodologies are developed for day-ahead applications. This requires day-ahead predictions of load demand and generation power as well as predictions related to EVs' SoC, time of arrival and time-of-departure. Yet, these predictions increase the uncertainty of the DS and reduce the robustness of NR. Therefore, the proposed real-time NR deals with these issues and defines the optimal topology of the MV DS by considering the real power transaction between the LV DSs and the MV DS.

The proposed methodology has several advantages. Firstly, the continuous update of the predictions improves the forecasting accuracy and enhances the robustness of the EV SCS methodology. Additionally, the proposed EV SCS methodology can effectively deal with the uncertainties related to the EVs'. Moreover, the residential controller adjusts the charging/discharging power of EVs and deals with the forecasting errors in real-time and alleviates their impact to the DS. Finally, the real-time NR of the MV DS complements the analysis and ensures the efficient operation of the overall DS, by considering the real-time power transactions between MV DS and LV DSs.

III. CASE STUDY

In this section the case study of the proposed methodology is presented. The simulation period is from 12:00 PM to 06:00 AM the next day, with a timestep of 15 minutes.

A. LV DS UNDER STUDY

The LV DS utilized in this paper consists of 108 buses, as presented in [12]. We assume that a household with a residential charger is connected to each bus. The daily load demand and PV power generation profiles of each household have been obtained from dataset [36]. This dataset includes half-hour active power demand and PV generation data from 300 households for a period of two years (01/07/2010 – 30/06/2012). Since DistFlow requires the reactive power as well, we calculate the reactive power, as presented in (24),

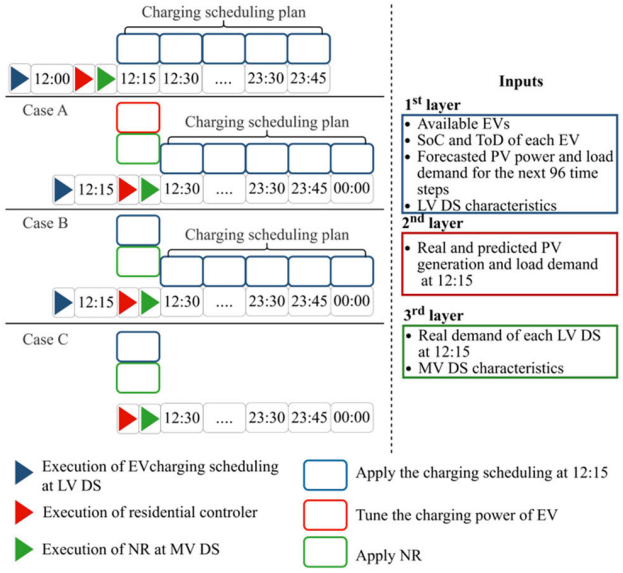

FIGURE 3. An example of two sequential executions of the proposed methodology.

considering that the power factor of the households is 0.97.

$$Q_{t,j,k}^{load,pred} = \tan(\cos^{-1}(pf_{i,k}) \cdot P_{t,j,k}^{load,pred} \quad (24)$$

Based on the location of each residence, hourly historical meteorological data (solar irradiation and temperature) are obtained from NASA POWER database [37]. Considering that the proposed methodology is applied to 15-min intervals, interpolation method is used to resample the time series and change the frequency of the data to 15-min.

B. LSTM FORECASTING MODELS

The LSTM forecasting models predict the PV generation and load demand of each household for the next 24 hours with a timestep of 15 minutes. The meteorological parameters used in the forecasting models have been obtained from POWER Data Access Viewer database considering the location of the households [37]. The data have been obtained with a recording frequency of 60-min. Therefore, interpolation method is employed to adjust the frequency to intervals of 15-min.

For the PV generation forecasts, 96 previous time steps of PV generation, solar irradiation, and temperature are used as inputs. Additionally, the load demand predictions are derived using as inputs the 96 previous values of the load demand, the ambient temperature, and the day of the week index. The selection of these variables is based on the results of a correlation analysis.

For each household the datasets of PV generation and load demand are divided into a 70% training set and a 30% test set. For the models' training MAE is selected as objective function, while Adam optimizer is used to optimize the weights of the predictor. Table 2 presents the parameters of the models, which are selected after trial-and-error process. Additionally, Figure 4 presents two indicative convergence plots for the training of a PV power and a load demand model.

The forecasting accuracy of the models is examined in terms of three indexes: a) MAE, b) NRMSE and c) MARNE [38].

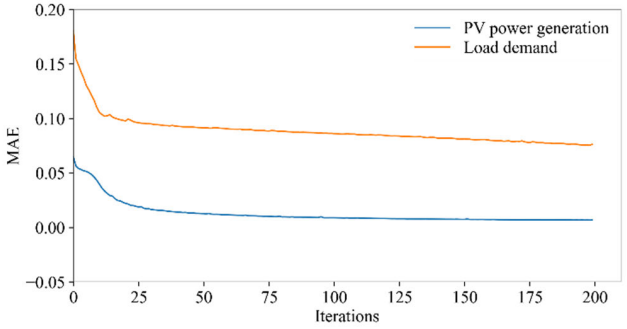

FIGURE 4. Convergence plots.

TABLE 2. Parameters of forecasting models.

Adam Optimizer	
Parameter	**Value**
Learning Rate	0.001
Beta1	0.9
Beta2	0.999
Momentum	0.99
Epsilon	1e-07
LSTM model	
Parameter	**Value**
Batch size	Training samples / 10
Epochs	200
Units	288
Activation function	ReLu

In this case study the MAEs serve as the forecasting error thresholds for the residential controllers. Specifically, the MAE of PV power and load demand of each household have been estimated and set as forecasting error threshold for that specific household.

C. EV DESCRIPTION

In this case study we consider that the EVs' penetration is 100%, i.e., an EV is connected to each household. Moreover, 19 EV models are utilized and are randomly assigned to the buses of the LV DS. The EV models, along with their battery capacities, are presented in [23]. Given that we are dealing with residential chargers, the EVs' parameters related to the maximum charging power, the time-of-arrival and the time-of-departure are defined accordingly. Specifically, the maximum charging power has been set at 7.6 kW, which coincides with the maximum rated power of the electrical installation, i.e., household.

Additionally, the time-of-arrival of the EVs is assumed to follow a normal distribution based on the EV travel partner presented in [39]. Specifically, the authors in [39] presented the daily EV charging load profiles based on demographics of vehicle users. Depending on the age of the vehicle owners, the arrival is from 16:00 to 18:00 for young aged people, while the arrival time of the elderly is distributed from 11:00 AM

to 06:00 PM. Hence, it is anticipated that the EVs arrive between 12:00 and 00:00, following a normal distribution. Moreover in [39] it is highlighted that the first trip is concentrated at around 7:00 AM during the workday. Thus, the time-of-departure in this case study is set at 06:00 AM of the next day. The time-of-departure and the final SoC are user defined parameters and can be set according to the EV owners' preferences.

The charging/discharging efficiency of each EV is set to 0.95. The initial SoC of the EVs upon arrival is randomly set between 20% and 40%, based on [40]. The authors in [40] assumed an initial SoC of EVs uniformly distributed between 10 - 40%. Considering this as well as the technical characteristics of the batteries, we defined the initial SoC within range 20% to 40%. Finally, it is assumed that all users want their EVs to be fully charged by the time of departure.

D. MV DS UNDER STUDY

The 33-bus IEEE system has been utilized for the analysis of the MV DS [12]. The first bus of the 33-bus system is the slack bus, while the rest ones are load buses. Considering the coupling between MV and LV DSs it is assumed that a LV DS, described in subsection III-A, is connected to each load bus of the MV DS. Therefore, a total of 3,456 households are connected to the MV DS.

Although the technical characteristics of the LV DSs are identical (length and impedance of lines), the assignment of households and EVs to the buses varies between them. Consequently, the total demand among the LV DSs differs.

The optimization of MV DS is based on a cost-worth analysis assessment including the cost from power losses reduction and the cost of the switching actions. To assess power loss benefits, day-ahead electricity prices from the ENTSO-E platform have been utilized. The data refer to Greece from 01/01/2023 to 02/01/2023 [41]. Additionally, the switching operation cost has been set equal to 0.5€ and it is taken from [42].

E. EXAMINED SCENARIOS

To assess the effectiveness of the proposed methodology and highlight the significance of addressing the coupling of MV and LV DSs, four scenarios have been formulated as follows:

- Sc#A: This is the base scenario where neither NR nor EV SCS is implemented.
- Sc#B: In this scenario, only EV SCS is applied at LV DSs. The purpose of this scenario is to examine how the SCS at LV DS contributes to the efficient operation and power flow mitigation at the MV DS.
- Sc#C: In this scenario, only NR is applied at MV DS.
- Sc#D: This scenario refers to the proposed methodology where the coupling of MV and LV DSs is considered.

IV. RESULTS

The proposed methodology is developed in a Python environment. The first and the third layers are formulated as a mathematical model using PYOMO, with Conopt and Bomin solvers selected for optimizing the LV DS and MV DS, respectively.

A. FORECASTING MODELS

The metrics of forecasting errors for PV generation and load demand for each residence are outlined in Table 3. These errors have been evaluated over the entire forecasting period, i.e., 96 timesteps ahead. Based on the forecasting results, we can conclude that the forecasting errors of PV generation are relatively lower than the load demand, while errors fluctuate among the households. These can be explained considering that: a) the load demand at residential level has higher uncertainty compared to the PV generation due to the stochastic behavior of end-users; and b) the efficiency of the forecasting models depends on the on the quality and relevance of the input data.

The MAEs presented in Table 3 serve as the forecasting error thresholds for the residential controllers and trigger the execution of SCS at the LV DS. It should be noted that these thresholds can be modified according to the users' preferences.

TABLE 3. MAE of forecasting models per residence.

PV power forecasting			
	MAE (kW)	NRMSE (%)	NRMSE (%)
#1	0.15	11.90	5.69
#2	0.29	14.77	6.54
#3	0.13	13.36	6.75
#4	0.25	12.93	5.72
#5	0.11	12.90	6.21
#6	0.15	11.39	5.66
Load forecasting			
MAE (kW)	MAE (kW)	MAE (kW)	MAE (kW)
#1	0.81	15.95	10.86
#2	0.53	11.14	7.19
#3	0.51	12.18	6.88
#4	0.48	10.66	6.42
#5	0.40	12.17	5.36
#6	0.45	10.64	6.19

B. LV DS ANALYSIS AND RESULTS

For the LV DS we consider both the application of the SCS and the residential controller. The performance of the controller is presented in Figure 5. The results refer to a specific timestep for 10 randomly selected houses of a LV DS. Figure 5a illustrates the real and forecasted load of the households. The load is defined as the residual demand or production in terms of net power for the residential installation, encompassing both PV generation and consumption. Figure 5b presents the initial and adjusted charging/discharging power of the EVs connected to the households.

At households #0, #2, #4, #6 and #8 the residential controller does not modify the charging power of EVs. This can be explained considering that the forecasting error does not

exceed the predefined threshold. However, in households #1, #3, #7 and #9 the residential controller adjusts the power to alleviate the impact of the forecasting error. In these cases, the controller adjusts the power to ensure that the total household consumption in real-time, depicted as "Load with controller adjustment" in Figure 5c, is equal to the total household consumption (SCS load) used in the SCS methodology. This alignment is crucial for maintaining the optimality of the SCS methodology and ensuring that real-time household consumption does not deviate from the scheduled consumption. In case the residential controller is omitted, this could result in high deviations between the real and scheduled consumption of households (Figure 5c).

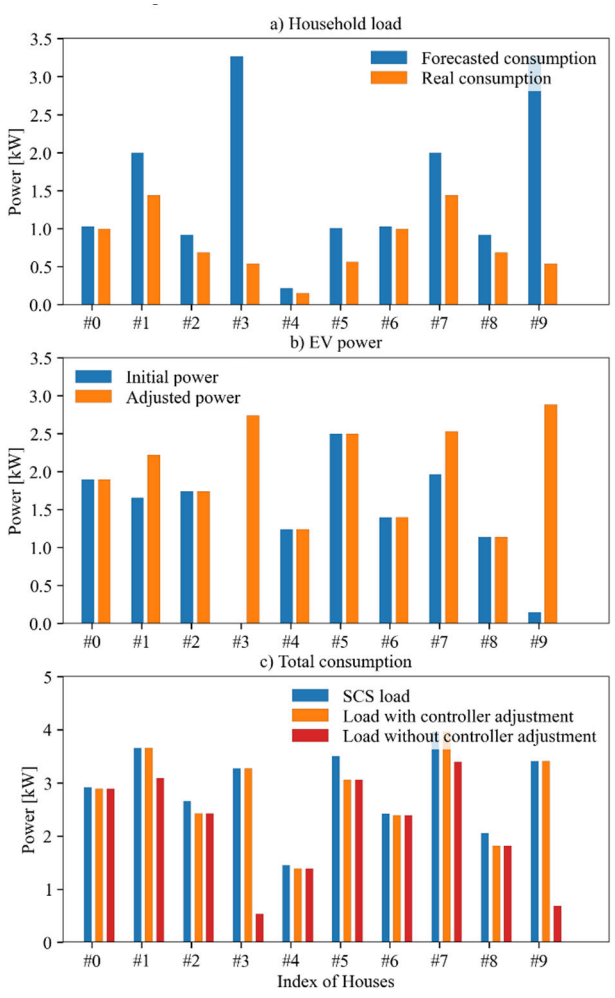

FIGURE 5. Performance of residential controller.

Figure 6 presents the load profiles and the Peak-Average Ratios (PAR) of one randomly selected household among the 32 LV DSs. The PAR is defined as the ratio of the peak demand to the average power consumption over a given period. From Figure 6a it is obvious that the uncontrolled charging of EV results in higher peaks and a lower PAR. In uncontrolled charging the EVs start charging with the maximum power, considering the limitations of the electrical installation (Figure 6b). Until the EV is fully charged, the total household's consumption is equal to the maximum rated power of the electrical installation (Figure 6a), i.e., 7.6 kW. On the contrary, the proposed SCS methodology can alleviate the peaks and significantly increase the PAR, leading to a smoother load profile.

The EV owners' preferences regarding the departure time and the final SoC are considered and satisfied. Figure 7 presents the SoC (Figure 7a) and the charging/discharging power (Figure 7b) of 108 EVs for the examined period. Additionally, Figure 7a includes information regarding the time of arrival, with the white color indicating that the EV is not plugged-in. Figure 7a highlights that the SoC at the time of departure is greater than 95%. Even when the EVs discharge (Figure 7b), they are fully charged by the time of their departure. The results in Figure 7 are indicative and refer to a randomly selected LV DS. However, the SoC and charging/discharging profiles of the rest LV DSs are quite similar.

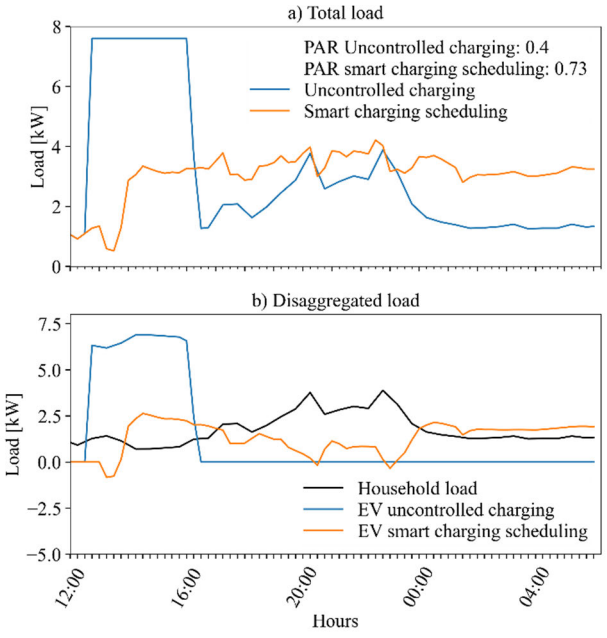

FIGURE 6. Household load profiles: a) total load, and b) household load and EV charging/discharging power.

The results of the SCS at the LV DSs are presented in the following figures. Specifically, Figure 8 presents the violin plots of the buses' voltage per LV DS. Each violin plot includes the voltage of the 108 buses for the total period of the analysis (72 quarters), i.e., 7.776 observations. In the uncontrolled charging (Figure 8a) most observations fall within 0.96 p.u. and 0.99 p.u., as presented by the statistics of the boxplots. Moreover, the distribution of the observations reveals a higher density around voltage values of approximately 0.98 p.u. Yet, the uncontrolled charging of EVs (Figure 8a) results in extreme voltage violations. There are voltage values lower than 0.90 p.u, meaning that the LV

DSs could not support 100% penetration of EVs without controlled charging. On the contrary, the employment of SCS (Figure 8b) improves the voltage profile of the buses. Across all LV DSs the lowest voltage remains above 0.9 p.u., while most of the voltage observations fall within 0.95 p.u. and 1.0 p.u. These conclusions are also evident in Table 4 which includes the ranges of the minimum and maximum voltage as well as the ranges of standard deviation among the 32 LV DS are presented in Table 4. Regarding the standard deviation it should be noted that it decreases slightly in case of SCS, ranging from 0.021 to 0.024, indicating more stable voltage levels.

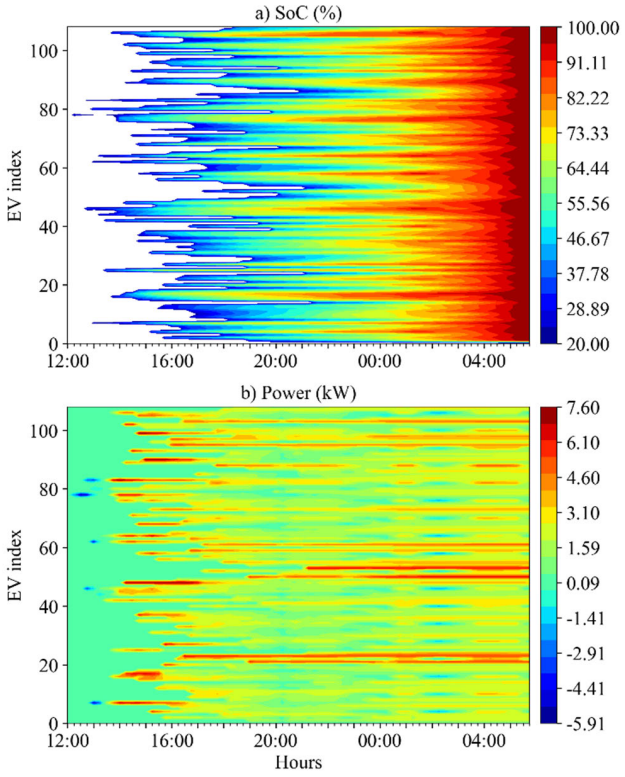

FIGURE 7. LV DS: a) charging profiles and b) SoC.

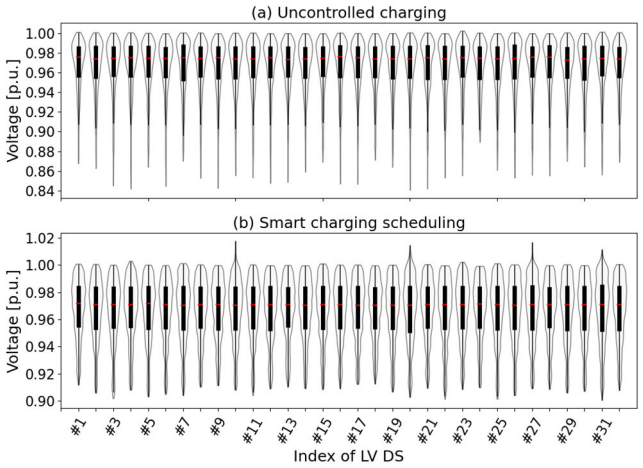

FIGURE 8. Violin plots of the buses' voltage per LV DS.

TABLE 4. Voltage and stability statistics: uncontrolled charging vs. smart charging scheduling.

Parameter	Uncontrolled charging	Smart Charging Scheduling
Minimum Voltage range (p.u.)	[0.84, 0.89]	[0.9, 0.91]
Maximum Voltage range (p.u.)	1	1
Standard deviation range	[0.25, 0.27]	[0.21, 0.24]

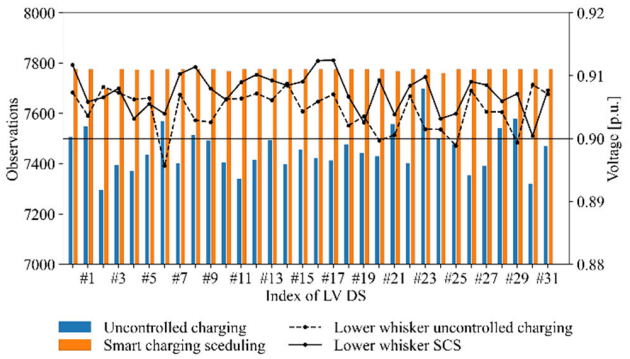

FIGURE 9. Number of observations included in the boxplots.

The violin plots do not include any information about the outliers, i.e., the extreme voltage dops observed during the day. Therefore, Figure 9 is also included providing additional information about the number of observations included in the boxplots and the values of the lower whisker. Regarding the former, from Figure 9 we can conclude that uncontrolled charging leads to a higher number of outliers compared to SCS, since the number of observations included in the boxplots is lower. Additionally, the values of the boxplots' lower whiskers are higher in the case of SCS and above 0.90p.u. in all cases. Based on Figures 8 and 9 we can conclude that SCS effectively mitigates the risk of extreme voltage drops and supports higher penetration of EVs.

Additionally, Figure 10 presents the power losses alongside PAR before and after the employment of the SCS. The uncontrolled charging results in PAR values close to 0.5. However, the employment of SCS can significantly increase the PAR up to almost 0.8. Additionally, the SCS mitigates the power losses among all LV DSs and can yield up to 22%, i.e.,1.2 MWh, total power losses reduction.

C. MV DS ANALYSIS AND RESULTS

The operation of the MV DS is affected by both NR and EV SCS. However, NR is applied only in Sc#C and Sc#D, while in Sc#A and Sc#B the MV DS has the initial topology and does not alternate. Table 5 provides a comprehensive overview of the operational details of switches, for Sc#C and Sc#D, focusing on the cost associated with power losses and the switching actions. The decision on whether to implement

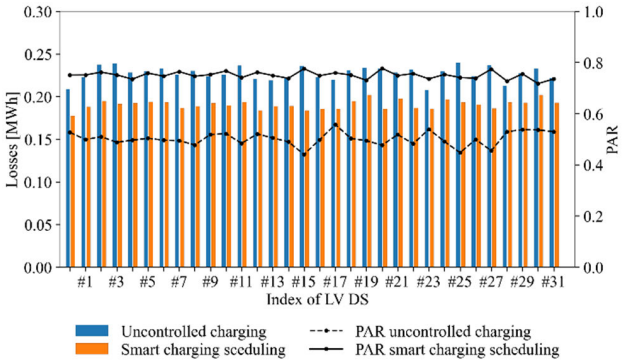

FIGURE 10. Power losses and par with and without the SCS.

NR or not is based on evaluating the energy cost related to losses before NR is applied and the combined cost of both energy losses and switching actions after NR is implemented. The operation of the switches varies between the two scenarios. When Sc#C is employed, the topology of the network changes three time within the day, i.e., 12:00, 12:15 and 16:00. However, when EV SCS is additionally employed (Sc#D) the switching actions are reduced. In this case the network is modified two times, at 12:00 and 12:15.

TABLE 5. Description of switching actions.

Sc	Hour	Parameter	Value
#C	12:00	Open switches	$S_{11\text{-}12}$, $S_{26\text{-}27}$, $S_{21\text{-}8}$, $S_{9\text{-}15}$, $S_{18\text{-}33}$
		Cost of losses before the NR (€)	13.27
		Cost of losses after NR (€)	10.23
		Cost of switching actions (€)	2
	12:15	Open switches	$S_{11\text{-}12}$, $S_{14\text{-}15}$, $S_{26\text{-}27}$, $S_{21\text{-}8}$, $S_{18\text{-}33}$
		Cost of losses before the NR (€)	17.09
		Cost of losses after NR (€)	14.72
		Cost of switching actions (€)	1
	16:00	Open switches	$S_{11\text{-}12}$, $S_{14\text{-}15}$, $S_{16\text{-}17}$, $S_{28\text{-}29}$, $S_{21\text{-}8}$
		Cost of losses before the NR (€)	89.37
		Cost of losses after NR (€)	84.22
		Cost of switching actions (€)	2
#D	12:00	Open switches	$S_{11\text{-}12}$, $S_{26\text{-}27}$, $S_{21\text{-}8}$, $S_{9\text{-}15}$, $S_{18\text{-}33}$
		Cost of losses before the NR (€)	12.58
		Cost of losses after NR (€)	9.71
		Cost of switching actions (€)	2
	12:15	Open switches	$S_{11\text{-}12}$, $S_{14\text{-}15}$, $S_{26\text{-}27}$, $S_{21\text{-}8}$, $S_{18\text{-}33}$
		Cost of losses before the NR (€)	15.61
		Cost of losses after NR (€)	13.42
		Cost of switching actions (€)	1

Additionally, the lines' loading, in terms of current, for each scenario is presented in Figure 11. Figure 11a illustrates that uncoordinated charging of EVs (Sc#A) can lead to significant increment of the lines' current. Additionally, when only NR is applied (Sc#C), the current of the first lines of the system during 15:00 and 19:00 may exceed 0.646 kA (Figure 11c). On the contrary, Figure 11b and Figure 11d show that applying SCS at the LV DSs alleviates the lines' current. Finally, the proposed methodology (Figure 11d) can further reduce the current of the lines compared to Sc#B (Figure 11b).

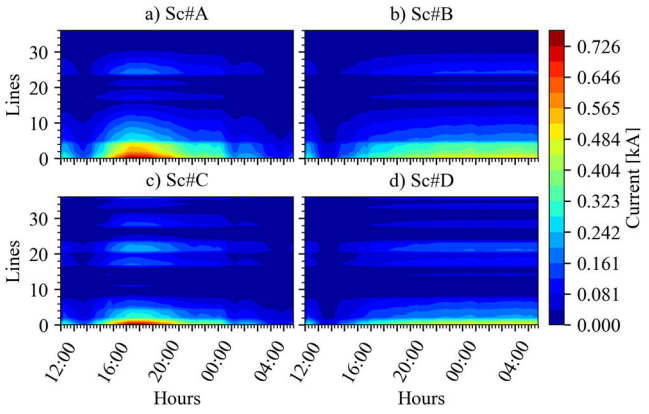

FIGURE 11. Heatmaps of line's current for: a) Sc#A, b) Sc#B, c) Sc#C and d) Sc#D.

The amount and cost of power losses at MV DS and LV DS for the examined scenarios are presented in Table 6. From Table 6, it is evident that that the proposed methodology (Sc#D) can significantly reduce the amount and cost of power losses compared to Sc#A, Sc#B and Sc#C. Specifically, the baseline scenario (Sc#A) has the highest amount and cost of power losses in both MV and LV DSs. When EV SCS (Sc#B) or NR (Sc#C) is applied, the total power losses of the DS are alleviated. Additionally, power losses at SC#B are reduced compared to Sc#C. Finally, the highest reduction is observed when Sc#D is employed, which can lead up to a 34.41% reduction in power losses compared to Sc#A.

TABLE 6. Amount and cost of power losses.

Parameter	Sc#A	Sc#B	Sc#C	Sc#D
MV DS losses (MWh)	16.44	14.23	10.38	9.46
LV DSs losses (MWh)	7.27	6.09	7.27	6.09
Total power losses (MWh)	23.71	20.32	17.65	15.55
Power losses reduction (%) in respect to Sc#A	-	14.29	25.55	34.41
MV DS power losses cost (€)	4980.37	3232.28	3140.18	2152.24
LV DSs power losses cost (€)	2194.96	1382.55	2194.96	1382.55
Total power losses cost (€)	7175.33	4614.83	5335.14	3534.79
Cost saving in respect to Sc#A (€)	-	2560.5	1840.19	3640.54

V. DISCUSSION AND LIMITATIONS

The results from the previous section underscore the potential of the proposed methodology as a comprehensive approach to

managing distribution systems (DS) under increasing electric vehicle (EV) penetration, particularly in real-time scenarios aimed at reducing power losses. Through the integration of model predictive control-based EV SCS and leveraging residential controllers effectively, significant opportunities arise for improving the LV DS operational characteristics. The implementation of residential controllers could significantly enhance the flexibility of EVs, enabling real-time forecasting error mitigation. Additionally, real-time NR could further improve the operation of MV DS. By utilizing real-time operational data, the NR could effectively deal with load demand uncertainties and provide an optimal system's topology considering the minimization of both power losses and switching actions cost.

The proposed methodology has limitations regarding its complexity. In this paper, the SCS was tested in a LV DS consisting of 108 households. The average computational time of the methodology was 5.6 min, which is significantly lower than the 15-min timestep set for this analysis. However, increasing the parameters such as the number of EVs and households will lead to higher complexity and longer execution times. Additionally, the average computational time of NR in the 33-bus system is 1.7 sec. However, in larger systems with more switches this time could be significantly increased, preventing the real-time application of NR.

VI. CONCLUSION

The DSs are currently facing significant challenges due to the high volatility of energy prices and the high uncertainty related to RES generation, load demand and EVs. This paper deals with these issues and proposes a real-time three-layer optimization methodology for power loss minimization considering the coupling between the MV and LV DSs. The proposed methodology optimizes the operation of the DSs by exploiting the flexibility of EVs and the benefits of NR. More specifically, at the first layer an EV SCS methodology is proposed and applied at a residential LV DS, aiming to minimize the power losses. The EV SCS is formulated considering the day-ahead predictions of PV power generation and load demand. To ensure the robustness of the EV SCS methodology the sliding window method is utilized, while the EV SCS is based on model predictive control method. At the second layer a real-time residential controller is applied to deal with the forecasting errors by adjusting the charging/discharging power of EVs accordingly. At the third layer a real-time NR methodology is employed at the MV DS based on a cost-worth analysis aiming at minimizing the cost related to power losses and switching actions. The proposed methodology is compared to three scenarios. The first scenario (Sc#A), where neither EV SCS nor NR is applied, serves as baseline. At the second (Sc#B) and third scenarios (Sc#C) only EV SCH and NR are applied, respectively. When Sc#B and Sc#C are employed the total power losses can be reduced up to 14.29% and 25.55%, respectively regarding Sc#A. Finally, the results highlight that the proposed methodology outperforms the rest of the scenarios since it could reduce the power losses up to 34.41%.

In future work, we aim to explore the deployment of the proposed method in a decentralized manner. This approach could significantly reduce computational time and enhance the applicability of the method across various LV DSs. Furthermore, future studies will focus on investigating more efficient NR methodologies to simplify the method and improve its effectiveness. The proposed methodology provides a foundation for future research to explore the formulation of incentives aimed at encouraging EV user participation in EV SCS schemes. This study has demonstrated the potential of the methodology in reducing operational costs. Building upon these results, future research could focus on developing EV SCS participation schemes specifically designed to reduce power losses, thereby motivating EV owners to participate actively in the proposed scheme.

REFERENCES

[1] *Council Regulation of on an Emergency Intervention to Address High Energy Prices*, document (EU) 2022/1854, Eur. Commission, 2022.

[2] *Directive of the European Parliament and of the Council of 13 Sep. 2023 on Energy Efficiency and Amending Regulation (EU) 2023/955 (recast)*, document (EU) 2023/1791, Eur. Commission, 2023.

[3] *2nd CEER Report on Energy Losses*, Council Eur. Energy Regulators, Brussels, Belgium, 2020.

[4] Eur. Union Agency for Cooperation Energy Regulators (ACER). (2019). *ACER Practice Report on Transmission Tariff Methodologies in Europe*. [Online]. Available: https://documents.acer.europa.eu/Official_documents/Acts_of_the_Agency/Publication/ACER

[5] *Communication From the Commission to the European Parliament, the Council, the European Economic and Social Committee and the Committee of the Regions, Digitalising the Energy System-EU Action Plan, SWD(2022) 341 Final*, Eur. Commission, 2022.

[6] *Report From the Commission to the European Parliament and the Council Promotion of E-mobility Through Buildings Policy*, Eur. Commission, Brussels, Europe, 2023.

[7] I. Saviuc, C. Lopez, A. Puskas, K. Rollert, and P. Bertoldi, "Explicit demand response for small end-users and independent aggregators," Publications Office Eur. Union, Luxembourg, Tech. Rep. EUR 31190 EN, JRC129745, 2022, doi: 10.2760/625919.

[8] S. Rafique, M. S. H. Nizami, U. B. Irshad, M. J. Hossain, and S. C. Mukhopadhyay, "EV scheduling framework for peak demand management in LV residential networks," *IEEE Syst. J.*, vol. 16, no. 1, pp. 1520–1528, Mar. 2022.

[9] A. Shahkamrani, H. Askarian-abyaneh, H. Nafisi, and M. Marzband, "A framework for day-ahead optimal charging scheduling of electric vehicles providing route mapping: Kowloon case study," *J. Cleaner Prod.*, vol. 307, Jul. 2021, Art. no. 127297.

[10] X. Fang, J. Li, Y. Yuan, and X. Yuan, "Decentralized control strategy for participation of electric vehicles in distribution voltage control," *Processes*, vol. 11, no. 9, p. 2552, Aug. 2023.

[11] A. Visakh and M. P. Selvan, "Analysis and mitigation of the impact of electric vehicle charging on service disruption of distribution transformers," *Sustain. Energy, Grids Netw.*, vol. 35, Sep. 2023, Art. no. 101096.

[12] D. Kothona and A. Bouhouras, "A two-stage EV charging planning and network reconfiguration methodology towards power loss minimization in low and medium voltage distribution networks," *Energies*, vol. 15, no. 10, p. 3808, May 2022.

[13] S. A. Mansouri, Á. Paredes, J. M. González, and J. A. Aguado, "A three-layer game theoretic-based strategy for optimal scheduling of microgrids by leveraging a dynamic demand response program designer to unlock the potential of smart buildings and electric vehicle fleets," *Appl. Energy*, vol. 347, Oct. 2023, Art. no. 121440.

[14] S. Zheng, G. Huang, and A. C. K. Lai, "Coordinated energy management for commercial prosumers integrated with distributed stationary storages and EV fleets," *Energy Buildings*, vol. 282, Mar. 2023, Art. no. 112773.

[15] S. Liang, B. Zhu, J. He, S. He, and M. Ma, "A pricing strategy for electric vehicle charging in residential areas considering the uncertainty of charging time and demand," *Comput. Commun.*, vol. 199, pp. 153–167, Feb. 2023.
[16] K. V. Sastry, D. G. Taylor, and M. J. Leamy, "Decentralized smart charging of electric vehicles in residential settings: Algorithms and predicted grid impact," *IEEE Trans. Smart Grid*, vol. 15, no. 2, pp. 1926–1938, Mar. 2024.
[17] M. H. Cedillo, H. Sun, J. Jiang, and Y. Cao, "Dynamic pricing and control for EV charging stations with solar generation," *Appl. Energy*, vol. 326, Nov. 2022, Art. no. 119920.
[18] B. Kandpal, P. Pareek, and A. Verma, "A robust day-ahead scheduling strategy for EV charging stations in unbalanced distribution grid," *Energy*, vol. 249, Jun. 2022, Art. no. 123737.
[19] X. Shi, Y. Xu, Q. Guo, H. Sun, and X. Zhang, "Day-ahead distributionally robust optimization-based scheduling for distribution systems with electric vehicles," *IEEE Trans. Smart Grid*, vol. 14, no. 4, pp. 2837–2850, Nov. 2022.
[20] S. Chen, Y. Liu, Z. Guo, H. Luo, Y. Zhou, Y. Qiu, B. Zhou, and T. Zang, "Deep reinforcement learning based research on low-carbon scheduling with distribution network schedulable resources," *IET Gener., Transmiss. Distribution*, vol. 17, no. 10, pp. 2289–2300, May 2023.
[21] Y. Jin, M. Amoasi Acquah, M. Seo, S. Ghorbanpour, S. Han, and T. Jyung, "Optimal EV scheduling and voltage security via an online bi-layer steady-state assessment method considering uncertainties," *Appl. Energy*, vol. 347, Oct. 2023, Art. no. 121356.
[22] L. Affolabi, M. Shahidehpour, F. Rahimi, F. Aminifar, K. Nodehi, and S. Mokhtari, "DSO market for transactive scheduling of electric vehicle charging stations in constrained hierarchical power distribution and urban transportation networks," *IEEE Trans. Transp. Electrific.*, early access, Apr. 10, 2023, doi: 10.1109/TTE.2023.3265912.
[23] A. S. Bouhouras, D. Kothona, P. A. Gkaidatzis, and G. C. Christoforidis, "Distribution network energy loss reduction under EV charging schedule," *Int. J. Energy Res.*, vol. 46, no. 6, pp. 8256–8270, May 2022.
[24] M. Nodehi, A. Zafari, and M. Radmehr, "A new energy management scheme for electric vehicles microgrids concerning demand response and reduced emission," *Sustain. Energy, Grids Netw.*, vol. 32, Dec. 2022, Art. no. 100927.
[25] J. Maeng, D. Min, and Y. Kang, "Intelligent charging and discharging of electric vehicles in a vehicle-to-grid system using a reinforcement learning-based approach," *Sustain. Energy, Grids Netw.*, vol. 36, Dec. 2023, Art. no. 101224.
[26] S. Zafar, A. Blavette, G. Camilleri, H. Ben Ahmed, and J.-J. Prince Agbodjan, "Decentralized optimal management of a large-scale EV fleet: Optimality and computational complexity comparison between an adaptive MAS and MILP," *Int. J. Electr. Power Energy Syst.*, vol. 147, May 2023, Art. no. 108861.
[27] E. Gumrukcu, J. R. A. Klemets, J. A. Suul, F. Ponci, and A. Monti, "Decentralized energy management concept for urban charging hubs with multiple V2G aggregators," *IEEE Trans. Transport. Electrific.*, vol. 9, no. 1, pp. 1736–1749, Sep. 2022.
[28] A. Maulik, "Probabilistic power management of a grid-connected microgrid considering electric vehicles, demand response, smart transformers, and soft open points," *Sustain. Energy, Grids Netw.*, vol. 30, Jun. 2022, Art. no. 100636.
[29] A. Maulik, "A hybrid probabilistic information gap decision theory based energy management of an active distribution network," *Sustain. Energy Technol. Assessments*, vol. 53, Oct. 2022, Art. no. 102756.
[30] H. Zhou, Y. Zhang, L. Yang, Q. Liu, K. Yan, and Y. Du, "Short-term photovoltaic power forecasting based on long short term memory neural network and attention mechanism," *IEEE Access*, vol. 7, pp. 78063–78074, 2019.
[31] L. Zhen, L. Zhang, T. Yang, G. Zhang, Q. Li, and H. Ouyang, "Simultaneous prediction for multiple source–loads based sliding time window and convolutional neural network," *Energy Rep.*, vol. 8, pp. 6110–6125, Nov. 2022.
[32] A. M. Nakiganda, S. Dehghan, and P. Aristidou, "Comparison of AC optimal power flow methods in low-voltage distribution networks," in *Proc. IEEE PES Innov. Smart Grid Technol. Eur. (ISGT Europe)*, Oct. 2021, pp. 1–5.
[33] T. J. Overbye, X. Cheng, and Y. Sun, "A comparison of the AC and DC power flow models for LMP calculations," in *Proc. 37th Annu. Hawaii Int. Conf. Syst. Sci.*, 2004, pp. 1–9.
[34] K. Purchala, L. Meeus, D. Van Dommelen, and R. Belmans, "Usefulness of DC power flow for active power flow analysis," in *Proc. IEEE Power Eng. Soc. Gen. Meeting*, Jun. 2005, pp. 1–6.
[35] C. Diaz, A. Mazza, F. Ruiz, D. Patino, and G. Chicco, "Understanding model predictive control for electric vehicle charging dispatch," in *Proc. 53rd Int. Universities Power Eng. Conf. (UPEC)*, Sep. 2018, pp. 1–6.
[36] *Solar Home Electricity Data*. Accessed: Jun. 20, 2023. [Online]. Available: https://www.ausgrid.com.au/Industry/Our-Research/Data-to-share/Solar-home-electricity-data
[37] *Power Data Access Viewer*. Accessed: Jun. 29, 2023. [Online]. Available: https://power.larc.nasa.gov/data-access-viewer/
[38] D. Kothona, I. P. Panapakidis, and G. C. Christoforidis, "Day-ahead photovoltaic power prediction based on a hybrid gradient descent and metaheuristic optimizer," *Sustain. Energy Technol. Assessments*, vol. 57, Jun. 2023, Art. no. 103309.
[39] J. Zhang, J. Yan, Y. Liu, H. Zhang, and G. Lv, "Daily electric vehicle charging load profiles considering demographics of vehicle users," *Appl. Energy*, vol. 274, Sep. 2020, Art. no. 115063.
[40] Y. Huo, F. Bouffard, and G. Joós, "An energy management approach for electric vehicle fast charging station," presented at the in *Proc. IEEE Electr. Power Energy Conf. (EPEC)*, Oct. 2017, pp. 1–15.
[41] *Entsoe Transparency Platform* Accessed: Feb. 2, 2023. [Online]. Available: https://transparency.entsoe.eu/dashboard/show
[42] Y. Gao, W. Wang, J. Shi, and N. Yu, "Batch-constrained reinforcement learning for dynamic distribution network reconfiguration," *IEEE Trans. Smart Grid*, vol. 11, no. 6, pp. 5357–5369, Nov. 2020.

DESPOINA KOTHONA (Student Member, IEEE) received the Dipl. (Eng.) degree from the Electrical Engineering Department, UTH, in 2020. She is currently pursuing the Ph.D. degree with the Electrical and Computer Engineering Department, University of Western Macedonia, Kozani, Greece. Her main research interests include optimal operation of distribution systems, optimal operation of PV systems, and development of efficient forecasting models. She has authored or co-authored 16 articles in these fields.

ANESTIS G. ANASTASIADIS received the Diploma degree in physics and the Diploma degree in electrical and computer engineering from the Aristotle University of Thessaloniki, Greece, in 1995 and 2004, respectively, the Diploma degree in economics from the School of Economic Science, Athens University of Economics, in 2016, the M.Sc. degree in thermal power, specializing in aerospace propulsion—gas turbine propulsion from Canfield University, U.K., in 2001, the M.Sc. degree in radio electronics (specialization: telecommunications) from the Faculty of Physics, Aristotle University of Thessaloniki, in 2001, the M.Sc. degree in applied economics and finance specializing in strategic decisions from Athens University of Economics, in 2013, the M.Sc. degree in technical projects management from Greek Open University, in 2022, and the Ph.D. degree from the National Technical University of Athens (NTUA), in 2014. He is currently pursuing the Diploma degree with the Department of Business Administration, Athens University of Economics. He is an Assistant Director with the Strategy and Research and Development Departments, Power Public Corporation S.A. His research interests include power system and power market analysis, renewable energy sources, economics issues of dispersed generation, electric vehicles, microgrids and smart grids, telecommunications issues, and power electronics and optimization methods. He has participated in more than 35 European research projects. He is a member of the Technical Chamber of Greece and CIGRE.

KOSTAS CHRYSAGIS received the master's degree in open and distance learning from Open University, the master's degree in leadership and negotiation from the Harvard Executive Program, AIT, and the Ph.D. degree in advanced predictive control strategies in the presence of uncertainty and systems with time delays from the University of Florida, USA. He is currently a Chemical Engineer with the National Technical University of Athens. He is also the Director of the EU Programs Coordination Department, Public Power Corporation S.A., the biggest energy producer and supplier in Greece. He holds more than 250 presentations in international conferences and project meetings and has more than 33 publications in international conference proceedings and scientific journals. He is a member of IEEE (Societies: Control, Robotics, and Cybernetics), American Institute of Chemical Engineers (AIChE), and the Technical Chamber of Greece; and a past member of EURON—EUROP (European Robotics Platform). Finally, he is an Expert Member of Vision2020 European Platform. He has coordinated more than 25 EU-funded projects, out of a total of more than 125 projects.

GEORGIOS C. CHRISTOFORIDIS (Senior Member, IEEE) received the Dipl. (Eng.) degree from the Electrical Engineering Department, AUTH, in 1998, the M.Sc. degree (Hons.) in power electronics and drives from the Electrical and Electronic Engineering Department, University of Birmingham, U.K., in 1999, and the Ph.D. degree from AUTH, in 2004. Since 2019, he has been with the Electrical and Computer Engineering Department, University of Western Macedonia, Kozani, Greece, as a Professor in power systems. His main research interests include distribution power networks, smart grids, integration of renewable energy sources, and EMC. He has authored or co-authored 157 articles in these fields.

AGGELOS S. BOUHOURAS (Member, IEEE) received the Dipl.-Eng. and Ph.D. degrees from the Department of Electrical and Computer Engineering, Aristotle University of Thessaloniki, in 2005 and 2010, respectively. Since 2019, he has been with the Electrical and Computer Engineering Department, University of Western Macedonia, Kozani, Greece, as an Associate Professor in electrical distribution systems. His main research interests include optimal operation of distribution systems, energy management systems, and non-intrusive load monitoring methodologies. He has authored or co-authored 89 articles in these fields.